

March 1998  
SLAC-PUB-7760  
LCLS-TN-98-1

# High Quantum Yield, Low Emittance Electron Sources

Jim Clendenin and G.A. Mullhollan

*Presented at the 15th ICFA Advanced Beam Dynamics Workshop,  
Quantum Aspects of Beam Dynamics, Monterey, CA, USA,  
January 4–9, 1998*

---

*Stanford Linear Accelerator Center, Stanford University, Stanford, CA 94309*

Work supported by Department of Energy contract DE-AC03-76SF00515.

## HIGH QUANTUM YIELD, LOW EMITTANCE ELECTRON SOURCES\*

J. E. Clendenin and G. A. Mulhollan

Stanford Linear Accelerator Center, Stanford, CA 94309

### Abstract

The upper limit for the rms normalized emittance is shown to be  $0.3 \times 10^{-6} \pi$  m per mm of radius for an electron beam extracted from a flat copper photocathode illuminated uniformly with 266-nm light. Using a III-V semiconductor such as GaAs, this limit can be reduced to  $0.1 \times 10^{-6} \pi$  m at room temperature and as low as  $0.05 \times 10^{-6} \pi$  m at cryogenic temperatures while maintaining a reasonable quantum yield. Semiconductor photocathodes in rf guns with an emittance compensation system are briefly compared with a new idea—a fast, pulsed, semiconductor photocathode closely coupled to an rf accelerating system.

*Presented at the  
15th ICFA Advanced Beam Dynamics Workshop  
Quantum Aspects of Beam Dynamics  
Monterey, CA USA, January 4-9, 1998*

---

\*Work supported by Department of Energy contract DE-AC03-76SF00515.

# HIGH QUANTUM YIELD, LOW EMITTANCE ELECTRON SOURCES\*

J. E. CLENDENIN AND G. A. MULHOLLAN

*Stanford Linear Accelerator Center  
Stanford University, Stanford, CA 94309  
E-mail: clen@slac.stanford.edu*

The upper limit for the rms normalized emittance is shown to be  $0.3 \times 10^{-6} \pi$  m per mm of radius for an electron beam extracted from a flat copper photocathode illuminated uniformly with 266-nm light. Using a III-V semiconductor such as GaAs, this limit can be reduced to  $0.1 \times 10^{-6} \pi$  m at room temperature and as low as  $0.05 \times 10^{-6} \pi$  m at cryogenic temperatures while maintaining a reasonable quantum yield. Semiconductor photocathodes in rf guns with an emittance compensation system are briefly compared with a new idea—a fast, pulsed, semiconductor photocathode closely coupled to an rf accelerating system.

## 1 Introduction

The generation of low emittance electron beams is increasingly important for accelerator applications. Extremely low emittances in both planes, important for linac-driven FELs<sup>1</sup> and certain collider designs,<sup>2</sup> can in principle be produced by rf photoinjectors.

RF photoinjectors with emittance compensation are one route to emittances on the order of  $10^{-6} \pi$  m. The uncorrelated emittance of the beam at the cathode, the so-called "thermal emittance," sets the lower limit of emittance that can be achieved. Thermal emittances are difficult to measure directly under the desired operating conditions for an rf photoinjector, viz., high charge density and high extraction field. Sec. 2 derives an expression for the upper limit of the transverse thermal emittance for a metal photocathode, while Sec. 3 discusses a method to measure the longitudinal thermal emittance of a photocathode in an rf gun based on the Schottky effect. Finally in Sec. 4, the significantly lower thermal emittance that is achievable with semiconductor photocathodes and the implications for source design is discussed, while Sec. 5 briefly discusses two methods to maintain low emittance when accelerating to high energy.

---

\*Also published as SLAC-PUB-7760, a publication of the Stanford Linear Accelerator Center. Work supported by Department of Energy contract DE-AC03-76SF00515.

## 2 Upper Limit of Thermal Emittance for Metal Photocathodes<sup>a</sup>

The normalized rms emittance,  $\epsilon_{rms}$ , can be defined by the expression

$$\epsilon_{n,rms} = \frac{1}{m_o c} \sqrt{\langle x^2 \rangle \langle p_x^2 \rangle - \langle x \cdot p_x \rangle^2} \quad (1)$$

where  $p_x$  is the x-component of the momentum.

At the cathode,  $\langle x \cdot p_x \rangle = 0$ , therefore

$$\epsilon_{n,rms} = x_{rms} \frac{p_{x,rms}}{m_o c}. \quad (2)$$

If  $r_o$  is the radius of the cathode, then for uniform emission  $x_{rms} = \frac{r_o}{2}$ .

In an rf gun, due to the Schottky effect,<sup>3</sup> the work function for a metal photocathode,  $\Phi$ , is changed by

$$-\Delta\Phi = e\Delta V = e\sqrt{\frac{eE_c}{4\pi\epsilon_o}} \quad (3)$$

upon application of the cathode extraction field,  $E_c = E \cos\theta_{ext}$ ,  $E$  being the maximum field at the cathode and  $\theta_{ext}$  the rf phase relative to the crest at the time the electrons are extracted.

The electrons are assumed to be emitted isotropically. At the surface, before emission, the maximum kinetic energy,  $E_{kin}$  is equal to the photon energy,  $E_{ph}$ . Thus if  $\phi$  is the azimuth angle, electrons can't penetrate the surface potential barrier if

$$\phi > \phi_{max} = \arccos \sqrt{\frac{\Phi_{eff}}{E_{kin}}}, \quad (4)$$

where  $\Phi_{eff} = \Phi - e\Delta V$ .

The momentum before emission is given by

$$p = m_o c \sqrt{\gamma^2 - 1} = m_o c \sqrt{\frac{2E_{kin}}{m_o c^2}} \quad (5)$$

for low energies. The x-component of momentum is given by

$$p_x = p \sin \phi \cos \theta \quad (6)$$

---

<sup>a</sup>The discussion here follows closely that of K. Flöttmann, TESLA-FEL 97-01 (Feb., 1997). However the actual problem discussed by Flöttmann concerned the thermal emittance of a semiconductor (Cs<sub>2</sub>Te) and did not invoke the Schottky mechanism.

where  $\theta$  is the meridian angle. The rms value of  $p_x$  can be found in the usual manner:

$$p_{x,rms} = \sqrt{\frac{\iint p_x^2 \sin \phi d\phi d\theta}{\iint \sin \phi d\phi d\theta}} = m_o c \sqrt{\frac{\epsilon E_{kin}}{m_o c^2}} \frac{1}{\sqrt{3}} \sqrt{\frac{2 + \cos^3 \phi_{max} - 3 \cos \phi_{max}}{2(1 - \cos \phi_{max})}} \quad (7)$$

where the integral in  $\theta$  is from 0 to  $2\pi$  and in  $\phi$  is from 0 to  $\phi_{max}$ .

Since  $p_x$  is not changed by the emission process, the final expression for the normalized rms emittance is

$$\epsilon_{n,rms} = \frac{r_c}{2} \sqrt{\frac{2E_{kin}}{m_o c^2}} \frac{1}{\sqrt{3}} \sqrt{\frac{2 + \cos^3 \phi_{max} - 3 \cos \phi_{max}}{2(1 - \cos \phi_{max})}}. \quad (8)$$

For clean Cu,  $\phi \sim 4.6$  eV at low voltage. If a laser tuned to 266 nm is used to illuminate the cathode surface, then  $E_{ph}$  is also  $\sim 4.6$  eV. Thus for  $E = 130$  MV/m and  $\theta_{ext} = 50^\circ$ ,  $\Delta V \sim 0.4$  eV and  $\phi_{eff} \sim 4.2$  eV, and thus  $\phi_{max} = 17^\circ$ ; i.e., all the electrons are emitted into a narrow cone perpendicular to the surface with a half angle of  $17^\circ$ . In this case  $\epsilon_{n,rms} \approx 0.3 \times 10^{-6} \pi$  m per mm radius.

This result is considered an upper limit because we have assumed that electrons approaching the surface have the maximum allowed momentum, whereas in fact there is a distribution of momenta since some electrons are promoted from well below the Fermi energy and since the effect of inelastic scattering is ignored. On the other hand, the effect of surface roughness,<sup>4</sup> which presumably increases the emittance, is also ignored here.

### 3 Thermal Emittance Based on Effective Temperature

For a relative small change in the work function,  $\Delta\Phi$ , the quantum efficiency<sup>b</sup> (QE) of a photocathode changes by:

$$\frac{QE}{(QE)_o} = e^{-\frac{\Delta\Phi}{kT_e}}, \quad (9)$$

where  $T_e$  is the effective temperature of the electron beam. The Schottky effect gives the variation in  $\Phi$  with the application of an external electric field. Thus if the  $QE$  as a function of the field on a cathode is measured, it is possible to deduce  $T_e$  using Eq. (9).

Substituting Eq. (3) for  $\Delta\Phi$  in Eq. (9) results in:

$$QE = (QE)_o e^{\frac{e}{kT_e} \sqrt{\frac{eE_c}{4\pi\epsilon_o}}}. \quad (10)$$

<sup>b</sup>The QE is defined as the ratio of emitted electrons to incident photons.

Table 1: Charge and assumed QE as a function of cathode field.

$E_c$ (MV/m)	Q (nC)	QE
33.6	0.178	$5 \times 10^{-6}$
118	0.400	$10^{-5}$

Pending a more detailed measurement with an rf gun of charge,  $Q$ , as a function of  $E_c$ , we can use the data from Fig. 4 of Palmer et al<sup>5</sup> which is summarized here in Table 1. The QE is not given in the reference, so in Table 1 the absolute value of the QE is based on independent measurements while the ratio of QEs is based on the measured charge. The exact absolute value has little effect on the results derived here.

The data of Table 1 is sufficient to calculate the slope,  $\beta$ , of the straight line obtained by plotting  $\ln(QE)$  versus  $E_c^{\frac{1}{2}}$ . The result is  $\beta = 0.14 \text{ (V/m)}^{-\frac{1}{2}}$ . Since

$$\frac{kT_e}{e} = \sqrt{\frac{e}{4\pi\epsilon_o}} \frac{1}{\beta}, \quad (11)$$

and since  $(\frac{e}{4\pi\epsilon_o})^{\frac{1}{2}} = 3.8 \times 10^{-5} \text{ (V/m)}^{-\frac{1}{2}}$ , it appears in this case that  $T_e = 0.27 \text{ eV}$ . Strictly speaking, this is a measure of the longitudinal effective temperature.

As a check on the validity of this approach, we can estimate the change in the work function as the cathode surface becomes oxidized. Let us assume the highest<sup>6</sup> measured QE reported in the literature for Cu at high fields and illuminated by 266-nm photons, about  $3 \times 10^{-4}$ , corresponds to a clean surface, whereas the lowest<sup>7</sup> QE measured under similar conditions, about  $5 \times 10^{-5}$ , corresponds to an oxidized surface. Then from Eq. 9,  $\Delta\Phi$  is about 0.5 eV for  $T_e = 0.27 \text{ eV}$ . For comparison, the maximum increase in  $\Phi$  associated with deposition of  $O_2$  on a clean Cu surface has been measured to be about 0.35 eV.<sup>8</sup>

Having found an effective temperature, we can calculate the corresponding thermal emittance from the classic relation for a thermionic cathode with uniform emission derived by Lawson.<sup>9</sup>

$$\epsilon_{n,rms} = \frac{\gamma r_c}{2} \sqrt{\frac{kT_e}{m_o c^2}}. \quad (12)$$

(The corresponding expression in Lawson is for the "effective" unnormalized emittance,  $\bar{\epsilon}$ , where  $\epsilon_{n,rms} = \beta\gamma\frac{\bar{\epsilon}}{4}$ .) For  $kT_e = 0.27 \text{ eV}$ , Eq. 12 yields  $\epsilon_{n,rms} = 0.35 \times 10^{-6} \pi \text{ m per mm radius}$ , which is strikingly similar to the upper limit

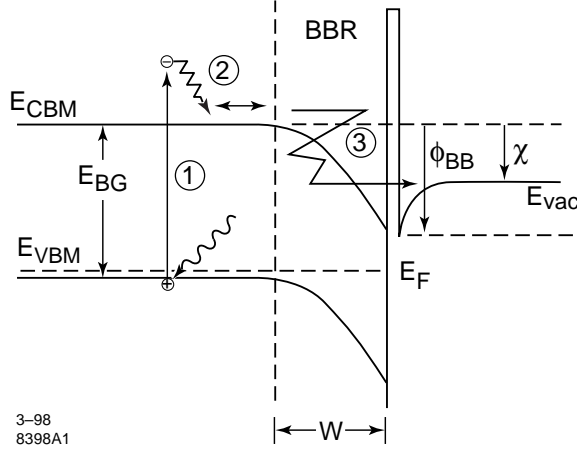


Figure 1: Schematic energy diagram near the surface for GaAs illustrating the three-step emission process where step 1 is absorption of a photon creating an electron-hole pair, step 2 is the thermalization and diffusion of the conduction band electron to the band bending region (BBR), and step 3 is the emission of the electron to vacuum.  $E_{VBM}$ ,  $E_{CBM}$ , and  $E_{vac}$  are valence band maximum, conduction band minimum, and vacuum level energies respectively.  $E_{BG}$  is the band gap,  $E_F$  the Fermi energy,  $\chi$  the electron affinity, and  $W$  and  $\phi_{BB}$  the width and depth of the BBR respectively.

calculated in Sec. 2. This result indicates that the effects of surface roughness may not be severe.

#### 4 Thermal Emittance of Semiconductors

Semiconductors are widely used as photocathodes because of their relatively high QE (10-30% for crystals  $\geq 1 \mu\text{m}$  thick) for excitation in the visible regime. The high QE derives primarily from the presence of a band gap (BG) separating the unfilled conduction band (CB) from the filled valence band (VB) of the semiconductor. The photoemission process in semiconductors can be understood in the framework of the three-step model<sup>10</sup> illustrated in Fig. 1: 1) absorption of photons in the bulk material resulting in promotion of electrons to the CB, (2) thermalization to the CB minimum (CBM) and transport of the CB electrons to the surface, and (3) escape of the surface electrons to vacuum. For GaAs at room temperature, the optical absorption depth,  $L_p = \alpha^{-1}$ , is typically on the order of  $1 \mu\text{m}$  for near-threshold excitation (photon energy

just greater than the BG energy,  $E_{BG}$ ), where  $\alpha$  is the optical absorption coefficient. If the photon energy with respect to the Fermi energy,  $E_F$ , is  $< 2E_{BG}$ , then the principal energy loss mechanism for the CB electron is by impurity or defect scattering and electron-phonon collisions, the latter being dominant for high-purity crystals. Inelastic electron-phonon collisions result in up to 50 meV energy loss per collision and a random change of direction of the electron momentum. Thus the transport process can be well described by diffusion theory. One reason for the high QE of bulk GaAs is that the diffusion length,  $L_D$ , in high-purity crystals is typically well matched to  $L_p$ . Here  $L_D = \sqrt{D\tau}$ , where  $D$  is the diffusion constant and  $\tau$  is the electronic lifetime in the bulk. Since the optical phonon mean free path at room temperature is only about 50 Å, the CB electrons arriving at the crystal surface are fully thermalized. (Thermalized electrons have an energy with respect to the CBM that is within the energy loss or gain of one electron-phonon collision.) Finally the surface escape probability is greatly enhanced by having a negative electron affinity (NEA) surface, which is obtained as follows. The work function for semiconductors can generally be reduced to be about equal to  $E_{BG}$  by depositing about a monolayer of cesium and an oxide (oxygen or fluorine) on the clean surface. Then for p-doped material, the energy bands are bent downward at the surface such that the vacuum energy,  $E_{vac}$ , is less than  $E_{CBM}$  in the bulk. For a dopant density  $> 10^{18} \text{ cm}^{-3}$ , band-bending can be as much as  $\frac{E_{BG}}{3}$  and the width of the band-bending region (BBR) is comparable to the photoelectron mean escape depth. For GaAs,  $E_{BG} \sim 1.4 \text{ eV}$  at room temperature.

Recently significant progress has been made by the Heidelberg group<sup>11</sup> to measure the mean transverse energy (MTE) of GaAs photoelectrons as a function of their longitudinal emission energy using a unique technique that seems to resolve several longstanding discrepancies. Their experimental longitudinal energy distribution curves of photoelectrons extracted from a GaAs (100) photocathode front-surface illuminated by 1.55 eV photons from a diode laser of constant intensity are shown in Fig. 2. For this data, the cathode was maintained fully activated with the vacuum level  $\sim 145 \text{ meV}$  below the CBM. Curves 1-5 were measured by progressively decreasing the electric field at the cathode with the aid of a grid while keeping the accelerating voltage constant (set by the bias of the cathode with respect to the grounded anode). When the electric field at the surface decreases, the vacuum level increases due to the diminishing Schottky effect. The curves can be understood as follows. Since in the bulk the CB electrons thermalize within about 10 nm, the emitted electrons with longitudinal energies  $> E_{CBM}$  are "hot" electrons (meaning high kinetic energy) that must have been promoted to the CB very near the surface. The maximum energy in Fig. 2 represents the VB-CB transition energy

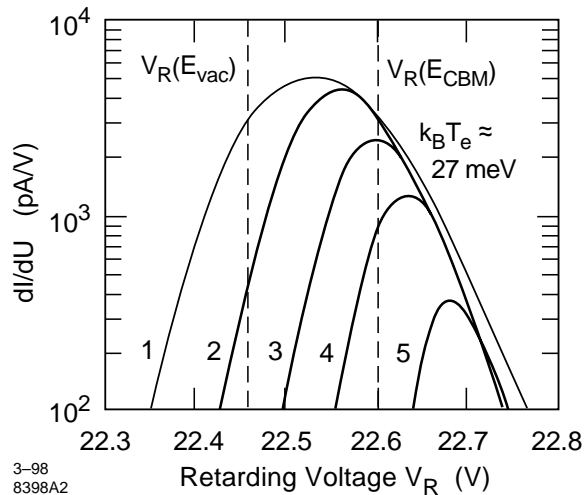
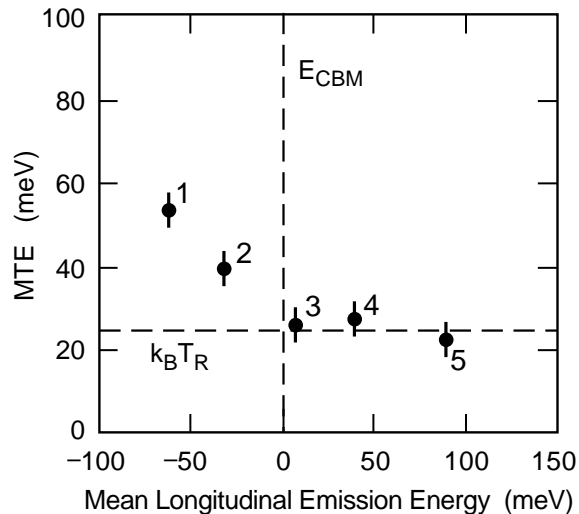


Figure 2: Longitudinal energy distribution curves from a fully (Cs,O)-activated cathode illuminated by 1.55 eV photons. Curves 1-5 correspond to decreasing extraction voltages. The negative electron affinity is  $\sim 145$  meV. (Adapted from Pastuszka et al., ref. 11.)

which is fixed for a given photon energy. Most of the electrons promoted to the CB arrive at the BBR fully thermalized. In the BBR they rapidly gain energies of up to  $\phi_{BB}$  as they approach the surface where typically they are either reflected or trapped in surface states. The reflected electrons lose energy as they undergo elastic collisions with phonons in the BBR which both prevents them moving back into the bulk and also causes them to heat up. ("Heat up" means randomization of momentum direction, i.e., an increase of the transverse component of momentum at the expense of the longitudinal.) The energy changes possible for an electron trapped in a potential well generally don't match the phonon energy, so trapped electrons lose energy (and heat up) relatively slowly.<sup>12</sup> Eventually some fraction of the electrons in the BBR which still have energies  $> E_{vac}$  are emitted into vacuum. As the vacuum level is increased, the low energy cut-off increases while the maximum energy remains constant as expected. The high-energy edge of the curves is Maxwellian and yields an effective longitudinal temperature of 27 meV.

The Heidelberg data for the increase in the MTE of emitted electrons as the mean longitudinal emission energy decreases below the CBM is shown in Fig. 3. Significantly, the MTE of the hot electrons is shown to be constant and equal to about 25 meV. This latter observation can be understood as follows.



3-98  
8398A3

Figure 3: Mean transverse energy (MTE) as a function of the mean longitudinal emission energy with respect to the conduction band minimum,  $E_{CBM}$ . (Adapted from Pastuszka et al., ref. 11.)

Upon initial promotion to the CB, the electrons retain the temperature of the acceptors in the VB, i.e., the temperature of the crystal itself,  $T_R$ , which in this case is room temperature, i.e.,  $\sim 25$  meV. Only fully ballistic hot electrons (i.e., electrons that have undergone no scattering) can be represented at the extreme high energy end of Fig. 3, so their measured MTE should correspond to the lattice temperature. However, some hot electrons have presumably undergone limited scattering causing them to lose energy and also to heat up. There is no evidence of these electrons in Fig. 3, which implies the number of such electrons that are emitted before their energy drops below  $E_{CBM}$  is relatively small. However, hot electrons initially promoted in the BBR itself also would have a longitudinal energy distribution covering the range of  $\phi_{BB}$  even without undergoing any scattering. Data points 3-5 in Fig. 3 are consistent with this mechanism.

Since the electron momentum parallel to the surface,  $k_{\parallel}$ , must be conserved during emission,<sup>c</sup> one would expect the MTE to be reduced by  $\frac{m_{eff}}{m_o}$  as electrons are emitted, where  $m_o$  is the electron mass in vacuum while  $m_{eff}$  is

<sup>c</sup>Strictly speaking,  $k_{\parallel}$  is conserved only for an infinitely extended periodic lattice.

the mass at the surface just before emission.<sup>13</sup> The MTE data of Fig. 3 above  $E_{CBM}$  implies  $m_{eff} \sim m_o$  despite the fact that the electron mass at the CBM for highly doped GaAs is only  $\sim 0.1 m_o$ . CB electrons with high kinetic energy in the  $\langle 100 \rangle$  direction (toward the surface) have a slightly increased  $m_{eff}$ , but nothing approaching  $m_o$ . The implication is that either the energy bands for the states near the surface have a different curvature due to modification of the bulk bands by reconstruction and the presence of the (Cs, oxide) overlayer, or the requirement that  $k_{\parallel}$  is conserved at the surface is effectively relaxed by surface imperfections.

The MTE shown in Fig. 3 was measured by the Heidelberg group using a unique method which allows the source to operate at high voltage and high charge. The cathode and beam transport to the detector is immersed in a relatively strong magnetic field,  $B$ , that overcomes the radial space charge forces. If the field between the source and the detector is adiabatically decreased, then some fraction of the transverse energy is transferred to the longitudinal degree of freedom since  $\frac{E_{\perp}}{B}$  is an adiabatic invariant. Keeping the field at the source ( $B_o$ ) constant, the MTE can be deduced by measuring the mean longitudinal energy for different ratios of  $\frac{B_f}{B_o}$ , where  $B_f$  is the field at the detector. The validity of this technique was first checked by measuring the MTE when a thermionic cathode was substituted for the semiconductor cathode.<sup>14</sup>

Using the data of Fig. 3 and Eq. (12), it is clear that very low thermal emittances—on the order of  $0.1 \times 10^{-6} \pi$  m per mm radius—are available using room temperature semiconductor cathodes (or even  $0.05 \times 10^{-6} \pi$  m for cryogenic temperatures), but only if  $E_{vac}$  is maintained at least as high as the CBM, i.e., only if the electron affinity is zero or positive. The QE for a zero affinity cathode is typically about a tenth that for the same cathode when it is fully NEA. Thus for a given electron beam intensity, an order of magnitude more laser energy is required. For extremely high electron beam intensities, the current density that can be extracted from the cathode is limited by a dynamic surface barrier that increases as the QE decreases.<sup>15</sup> However, a high dopant concentration seems to significantly reduce this effect<sup>16</sup> or possibly even eliminate it.<sup>17</sup>

## 5 Low Emittance Beams

For high intensities, space charge forces cause the emittance of a low-energy electron beam to rapidly increase. However, if the beam is accelerated while maintaining laminar motion, it has been shown that the growth in the emittance can be reversed and in effect the original uncorrelated emittance at the cathode restored at a point downstream where the energy is sufficiently high

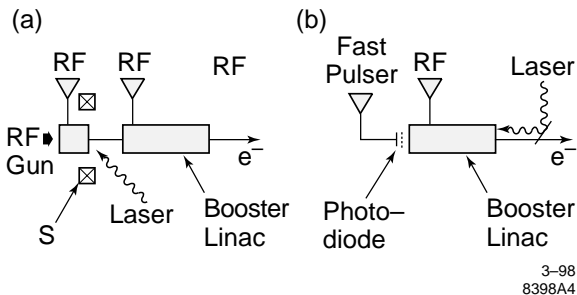


Figure 4: Simple schematics illustrating two methods to control the emittance of an electron beam: (a) rf photoinjector where S is the emittance-compensation solenoid; and (b) fast-pulsed photodiode closely coupled to booster accelerator.

that space charge is no longer a significant factor.<sup>18</sup> This scheme, which is illustrated in Fig. 4a, utilizes an rf gun with a surrounding emittance-compensation solenoid followed by a booster accelerator. The emittance at the exit of the booster accelerator is the quadratic sum<sup>19</sup> of the thermal emittance and the residual emittance growth in the accelerating system. With sufficient refinement, emittances from such a system might eventually be reduced to the level that the thermal emittance at the cathode becomes a limiting factor. Experimentally however it has proven difficult to reduce the rms normalized emittance for a 1 nC beam to below  $\sim 2 \times 10^{-6} \pi$  m per mm radius.<sup>20</sup>

Recently, very low emittances have been reported using a photocathode in a pulsed diode with extraction fields on the order of several GV/m<sup>21</sup> preceded by a 3-ns laser pulse with spot sizes on the cathode of 55-380  $\mu$ m FWHM. Cathode-anode spacings on the order of 1 mm were used, resulting in a beam energy of several MeV. The measured normalized rms emittances scale to  $\sim 0.5 \times 10^{-6} \pi$  m for 1 nC of charge with the pulse length of  $\sim 100$  ps set by the duration of the high voltage pulse.<sup>d</sup> (MAFIA simulations by Srinivasan-Rao et al.<sup>22</sup> for 1 nC of charge and a laser diameter and length of 100  $\mu$ m and 10 ps respectively indicate that for extraction fields on the order of 1 GV/m, it is possible to maintain emittances on the order of  $0.6 \times 10^{-6} \pi$  m even after a drift of 7 mm.) Such a diode might be incorporated into a low emittance electron source by positioning it at the entrance to a booster accelerator as shown in Fig. 4b. Potentially such a system does not require emittance compensation to achieve very low normalized emittances at high energies.

<sup>d</sup>Significantly shorter electron pulses may be possible if a shorter laser pulse is used.

## 6 Conclusions

Thermal emittances may prove to be the limiting factor for increasing the brightness of electron sources employing photocathodes. It has been shown here that semiconductor photocathodes have a significantly lower thermal emittance and higher QE than metal cathodes. Low emittance beams are now widely produced using rf photocathode guns employing emittance compensation techniques. Pulsed photodiodes closely coupled to rf accelerators may in the future provide an even brighter source without the need for emittance compensation.

## Acknowledgements

The authors would like to thank J. C. Sheppard for his encouragement to pursue these topics and for useful discussions.

## References

1. M. Cornacchia et al., SPIE 2988 (1997) 2.
2. V. Telnov, "Physics goals and parameters of photon colliders," Budker INP 98-02 (January, 1998), presented at the *2nd Int. Workshop on Electron-Electron Interactions at TeV Energies*, Santa Cruz, CA, Sept. 22-24, 1997.
3. S.M. Sze, *Physics of Semiconductor Devices* (New York, John Wiley, 1981), p. 251.
4. D.J. Bradley et al., J. Phys. D: Appl. Phys. 10 (1977) 111.
5. D.T. Palmer et al., "Emittance Studies of the BNL/SLAC/UCLA 1.6 cell Photocathode Gun," SLAC-PUB-7422 (1997), presented at the *1997 Particle Accelerator Conference*, May 12-16, 1997, Vancouver, BC.
6. E. Chevally et al., Nucl. Instrum. and Meth. A 340 (1994) 146.
7. X.J. Wang et al., Proc. of the *1995 Particle Accelerator Conference*, p. 890.
8. C.A. Papageorgopoulos, Phys. Rev. B 25 (1982) 3740.
9. J.D. Lawson, *The Physics of Charged-Particle Beams*, Clarendon Press, Oxford, 1988, p. 210.
10. W.E. Spicer, Phys. Rev. 112 (1958) 114.
11. S. Pastuszka et al., Appl. Phys. Lett. 71 (1997) 2967.
12. A.V. Subashiev, St. Petersburg Technical University, private communication.
13. G. Vergara et al., J. Appl. Phys. 80 (1996) 1809.

14. S. Zwickler et al., Proc. of the *Workshop on Photocathodes for Polarized Electron Sources for Accelerators*, SLAC-432 Rev. (1994), p. 445.
15. M. Woods et al., J. Appl. Phys. 73 (1993) 8531.
16. H. Tang et al., *4th European Particle Accelerator Conference*, May 17-23, 1994, London, UK (World Scientific, Singapore, 1994), p. 46.
17. T. Nakanishi et al., *7th Int. Workshop on Polarized Gas Targets and Polarized Gas Beams*, Aug. 18-22, 1997, Urbana-Champaign, IL, AIP Conf. Proceedings 421 (1998), p. 300.
18. B.E. Carlsten, Nucl. Instrum. and Meth. A 285 (1989) 313.
19. R.L. Sheffield et al., Nucl. Instrum. and Meth. A318 (1992) 282.
20. J. Clendenin, Proc. of the *XVIII Int. Linac Conference*, Aug. 26-30, 1996, Geneva, CH, p. 298.
21. F. Villa, *Advanced Accelerator Concepts Seventh Workshop*, AIP Proceedings 398 (1997), p. 739; also F. Villa and A. Luccio, "Test of a High-Gradient Low-Emittance Electron Gun," submitted for publication (1996).
22. Srinivasan-Rao et al., *Advanced Accelerator Concepts Seventh Workshop*, AIP Proceedings 398 (1997). p. 730.